ELSEVIER

Contents lists available at ScienceDirect

# Journal of Non-Crystalline Solids

journal homepage: www.elsevier.com/locate/jnoncrysol



#### Comment

# Prediction of the Young's modulus of silicate glasses by topological constraint theory



Kai Yang<sup>a</sup>, Benjamin Yang<sup>a</sup>, Xinyi Xu<sup>a</sup>, Christian Hoover<sup>b</sup>, Morten M. Smedskjaer<sup>c</sup>, Mathieu Bauchy<sup>a</sup>,\*

- <sup>a</sup> Physics of AmoRphous and Inorganic Solids Laboratory (PARISlab), University of California, Los Angeles, CA 90095, USA
- <sup>b</sup> School of Sustainable Engineering and the Built Environment, Arizona State University, Tempe, AZ 85287, USA
- <sup>c</sup> Department of Chemistry and Bioscience, Aalborg University, 9220 Aalborg, Denmark

#### ARTICLE INFO

Keywords: Stiffness Young's modulus Topological constraint theory Molecular dynamics Silicates

#### ABSTRACT

Understanding and predicting the compositional dependence of the stiffness of silicate glasses is key for various technological applications. Here, we propose a new topological model for predicting the Young's modulus of silicate glasses. We show that the Young's modulus is governed by the volumetric density of bond-stretching and bond-bending topological constraints acting in the atomic network. The predicted Young's modulus values offer an excellent agreement with molecular dynamics and experimental data over a wide domain of compositions (the entire calcium aluminosilicate ternary system) and a large range of Young's modulus values (from around 80 to 160 GPa).

#### 1. Introduction

Discovering new glasses with improved mechanical properties is key to address present and future challenges in energy, communication, and infrastructure [1–4]. Among all the mechanical properties that are of interest to glasses, the Young's modulus (*E*) plays a critical role in the performance of glass fibers [5–7]. More generally, the Young's modulus of glasses is an important engineering property for a large range of applications, including flexible substrates and roll-to-roll processing of displays, architectural glazing, ultra-stiff composites, hard discs and surgery equipment, or lightweight construction materials [1,8–10].

Accelerating the discovery of novel glasses with tailored functionalities requires the development of new predictive models that decipher the linkages between glass composition and properties [11]. To this end, several studies have attempted to derive a relationship between glass composition and Young's modulus. Thanks to its elegance and simplicity, the Makishima–Mackenzie (MM) model may be the most popular model to date [12,13]. This model is based on the idea that the Young's modulus of silicate glasses can be expressed as a linear combination of the dissociation energies of its oxide constituents, normalized by the atomic packing density. Although the predictions offered by the MM model are remarkably accurate considering the simplicity of this model, it is essentially an additive model assuming that the contributions of each oxide to the Young's modulus are proportional to

their concentration. However, the Young's modulus often shows a nonlinear dependence on composition, which cannot be captured by purely additive models [14,15]. More generally, the failure of the MM model to properly predict the non-linear relationship between composition and Young's modulus is likely due to the fact that this model does not embed any information about the atomic structure of glasses and the compositional dependence thereof [16].

As an alternative route, topological constraint theory (TCT) offers a promising route to predict the properties of glasses based on the topology of their atomic network [17-24]. TCT reduces complex disordered atomic networks into simpler mechanical trusses, wherein some nodes (the atoms) are connected to each other via some constraints (the chemical bonds). In molecular glasses, such constraints comprise: (i) the radial 2-body bond-stretching (BS) constraints that keep the bond lengths fixed around their average values and (ii) the angular 3-body bond-bending (BB) constraints that fix the average values of the interatomic angles. As such, TCT captures the connectivity of the glass network while filtering out second-order structural details that do not significantly affect macroscopic properties. Based on this framework, glasses are classified as flexible, stressed-rigid, or isostatic when the total number of BS and BB constraints per atom  $(n_c)$  is lower, larger, or equal to 3, respectively, which is the number of degrees of freedom per atom.

Within the framework of TCT, glasses can be considered as a

E-mail address: bauchy@ucla.edu (M. Bauchy).

<sup>\*</sup> Corresponding author.

network of atoms that are connected to each other via some "small springs" (the interatomic mechanical constraints)—so that the macroscopic stiffness of glasses should be related to the number of interatomic constraints. This echoes some results obtained by Thorpe for model random networks, wherein the stiffness was found to be zero in flexible systems ( $n_{\rm c} < 3$ ) and, subsequently, to scale with  $n_{\rm c}$  in stressed-rigid systems ( $n_{\rm c} > 3$ ) [25]. A similar relationship was observed in amorphous semiconductors [26–29] and chalcogenide glasses [16]. However, no topological model predicting the stiffness of ionocovalent silicate glasses is available to date.

Here, based on high-throughput molecular dynamics (MD) simulations of calcium aluminosilicate (CAS) glasses, we present a new topological model predicting the compositional dependence of the Young's modulus of silicate glasses. We demonstrate that our topological model offers realistic predictions of Young's modulus values over the entire CAS ternary domain.

#### 2. Simulation methods

To establish our conclusions, we conduct some high-throughput MD simulations of 231 CAS glasses. The chosen compositions homogeneously cover the CAS ternary domain, with 5% increments in the mol% concentration of the CaO, Al<sub>2</sub>O<sub>3</sub>, and SiO<sub>2</sub> oxide constituents. Note that, in practice, some of these systems would likely not exhibit satisfactory glass-forming ability. All the simulations are conducted using the Large-scale Atomic/Molecular Massively Parallel Simulator (LAMMPS) package [30]. Each system comprises around 3000 atoms. Since the quality of MD simulations mostly relies on that of the underlying force field, we adopt here the interatomic potential parametrized by Jakse [31,32]—as this potential has been shown to offer a realistic description of the mechanical properties of CAS glasses [15,33–35]. A cutoff of 8.0 Å is used for the short-range interactions. The Coulombic interactions are calculated by adopting the Fennell damped shifted force model with a damping parameter of  $0.25 \, \text{Å}^{-1}$  and a global cutoff of 8.0 Å [36]. The integration timestep is 1.0 fs.

The CAS glasses are prepared by quenching liquids, as described in the following [37]. First, some atoms are randomly placed in a cubic box using the PACKMOL package while using a distance cutoff of 2.0 Å between each atom to avoid any unrealistic overlap [38]. These initial configurations are then subjected to an energy minimization, followed by some 100 ps relaxations in the canonical (NVT) and isothermal-isobaric (NPT) ensembles at 300 K, sequentially. These samples are then melted at 3000 K for 100 ps in the NVT and, subsequently, NPT ensemble (at zero pressure) to ensure the loss of the memory of the initial configurations and to equilibrate the systems. Next, these liquids are cooled from 3000 to 300 K in the NPT ensemble at zero pressure with a cooling rate of 1 K/ps. The obtained glass samples are further relaxed at 300 K for 100 ps in the NPT ensemble before the stiffness computation. Note that this quenching procedure is slightly adjusted for select compositions. First, a higher initial melting temperature of 5000 K is used for the samples wherein the  $SiO_2$  concentration is larger or equal to 95 mol%—since these glasses exhibit high glass transition temperatures. Second, a faster cooling rate of 100 K/ps is used for the samples wherein the CaO concentration is larger or equal to 90 mol%. Indeed, although the cooling rate can affect the glass stiffness, the use of a higher cooling rate here is necessary as these systems would otherwise tend to crystallize with a cooling rate of 1 K/ps. Once formed and equilibrated, the glasses are subjected to a series of 6 deformations (i.e., 3 axial and 3 shear deformations along the 3 axes). Their stiffness tensor (and Young's modulus) is computed from the curvature of the potential energy (see Refs. [15, 33, 39, 40] for more details). Based on Ref. [15], the computed Young's modulus values are rescaled by a constant factor (0.86) to enhance the overall agreement with experimental data. The relative uncertainty of the simulated Young's modulus values (  $\pm$  2.5%) is estimated by computing the stiffness of 6 independently-quenched glasses for select compositions and calculating their standard deviation.

The coordination number of each atom is computed by enumerating the number of neighbors present in its first coordination shell—wherein the radius cutoff is defined as the minimum after the first peak of the partial pair distribution function (i.e., 2.00, 2.35, and 3.05 Å for Si-O, Al-O, and Ca-O, respectively).

#### 3. Topological model of Young's modulus

Our topological model is inspired by that developed by Smedskjaer, Mauro, and Yue, wherein hardness is expressed as a linear function of the number of constraints per atom  $n_{\rm c}$  [22,41–43]. Here, since the Young's modulus has the dimension of an energy per unit of volume, we postulate that E can be expressed in terms of the volumetric density of the energy created by each constraint. A similar approach was used to refine the original Smedskjaer model to predict hardness [44]. Further, we postulate that the BS and BB constraints do not contribute with equal weight to increasing the Young's modulus, which arises from the fact that BS and BB constraints exhibit different free energies and that different types of constraints may be activated under different loading conditions [23,45,46]. Based on these considerations, we propose the following model:

$$E = \varepsilon_{\rm BS} n_{\rm BS} + \varepsilon_{\rm BB} n_{\rm BB} \tag{1}$$

where  $n_{\rm BS}$  and  $n_{\rm BB}$  are the volumetric density of BS and BB constraints, respectively, and  $\varepsilon_{\rm BS}$  and  $\varepsilon_{\rm BB}$  are some fitting parameters that correspond to the typical energies of BS and BB constraints, respectively. This model assumes that a fictitious glass comprising no BS and BB constraints would have a zero Young's modulus. Note that, although Eq. (1) expresses E as a linear function, some degree of non-linearity can be captured in the number of topological constraints created by the atoms or the volumetric density of atoms.

#### 4. Results and discussion

### 4.1. Constraints enumeration

To assess the validity of our topological model, we first enumerate the number of BS and BB constraints in CAS glasses as a function of composition. In fully-connected covalent glasses, the number of BS constraints created by a given atom is given by r/2, where r is the coordination number-where the factor 2 arises from the fact that each BS constraint is shared by two atoms [17]. In turn, the number of BB constraints is usually given by 2r - 3, which corresponds to the number of independent angles that need to be fixed to define the angular environment of the atom [17]. However, due to the existence of ionic nondirectional bonds, this counting scheme does not always apply to ionocovalent silicate glasses [46]. As such, to avoid relying on any guesses in the enumeration of the constraints, we analyze the structure of the simulated glasses to directly extract the number of BS and BB constraints [19,46,47]. To this end, we compute the coordination number of each atom. We then identify the different types of O species present in the network, namely, (i) bridging-oxygen (BO), i.e., connected to 2 network formers (Si or Al), (ii) non-bridging oxygen (NBO), i.e., connected to only 1 network former, (iii) "tricluster" oxygen (TO), i.e., connected to 3 network formers [33,48], and (iv) "free oxygen" (FO), i.e., connected to 0 network formers (i.e., only connected to Ca

Table 1 summarizes the average number of BS and BB constraints created by each atomic species. In details, we find that, as expected, Si atoms systematically create 4 BS and 5 BB constraints with their 4 O neighbors—note that, for simplicity, the BS constraints are here fully attributed to the cations. Although some fraction of over-coordinated Al atoms is found in Al-rich glasses, most of them create 4 BS and BB constraints with their 4 O neighbors. Due to the ionic nature of Ca—O bonds, the constraints enumeration is trickier for Ca atoms. First, these atoms do not form any well-defined angular environment and, as such,

**Table 1** Summary of the average number of bond-stretching (BS) and bond-bending (BB) constraints created by each atomic species in  $(CaO)_x(Al_2O_3)_y(SiO_2)_{1-x-y}$  glasses. Note the BS constraints are here fully attributed to the cations. The quantities  $r_{Ca-NBO}$  and  $r_{Ca-FO}$  refer to the average number of non-bridging oxygen (NBO) and free oxygen (FO) atoms around each Ca atom.

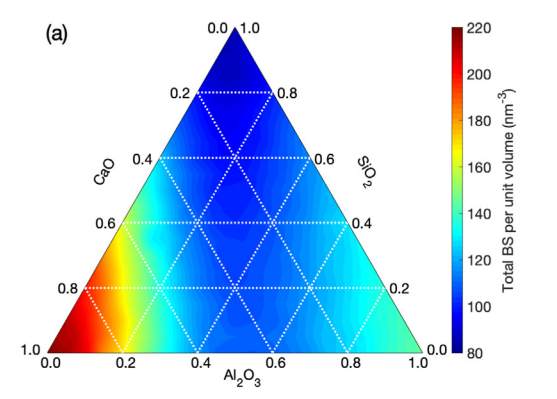
Species	Fraction	BS	BB
Si	1-x-y	4	5
Al	2y	4	5
Ca	x	$r_{\mathrm{Ca-NBO}} + r_{\mathrm{Ca-FO}}$	0
0	2 - x + y	_	_
FO		_	0
NBO		_	0
ВО		_	1
TO		-	3

do not create any BB constraints [47]. Second, a statistical analysis between the Young's modulus and the partial coordination number of Ca atoms reveals that Ca atoms only create BS constraints with their surrounding NBO and FO atoms [47]. In turn, Ca atoms do not create any constraints with the surrounding BO and TO atoms. This can be understood from the fact that the charge of BO and TO atoms is already fully compensated by those of their surrounding Si and Al neighbors, so that their interaction between Ca and BO/TO atoms is weaker than that between Ca and NBO/FO atoms. Finally, we find that, as expected, BO create 1 BB constraint, while TO atoms create 3 BB constraints to define their trigonal environment. In contrast, due to the ionic nature of Ca—O bonds, NBO and FO atoms do not create any BB constraint. These inputs then serve to compute the volumetric densities of BS and BB constraints ( $n_{\rm BS}$  and  $n_{\rm BB}$  in Eq. (1)).

Fig. 1 shows the volumetric densities of BS and BB constraints as a function of composition in the CAS ternary system. Overall, we find that the densities of BS and BB constraints primarily depends on the [CaO]—[Al $_2$ O $_3$ ] molar difference. In details, we find that the density of BS constraints is minimum when [CaO]—[Al $_2$ O $_3$ ] and increases in the Ca-and Al-rich domains. This arises from the fact that both of these domains exhibit a high average coordination number—i.e., due to the presence of 6-fold coordinated Ca atoms in Ca-rich glasses and TO atoms in Al-rich glasses [15]. On the other hand, the density of BB constraints presents a significantly different compositional dependence as it monotonically decreases with increasing [CaO]—[Al $_2$ O $_3$ ] molar difference. This arises from the fact that Ca atoms do not create any BB constraints, whereas TO atoms contribute to increasing the number of BB constraints in Al-rich glasses.

#### 4.2. Prediction of Young's modulus

We then focus on the compositional dependence of the Young's modulus (*E*) values computed by MD (see Fig. 2a). Overall, we observe



the existence of two main trends: (i) E tends to increase with decreasing SiO<sub>2</sub> concentration and (ii) E tends to increase with increasing [CaO]—[Al<sub>2</sub>O<sub>3</sub>] molar difference. However, we find that the compositional dependence of E is non-monotonic and that CaO and Al<sub>2</sub>O<sub>3</sub> exhibit some coupled effects. For example, we find that E increases with increasing CaO concentration when [Al<sub>2</sub>O<sub>3</sub>] = 0 mol%, whereas E decreases with increasing CaO concentration when [Al<sub>2</sub>O<sub>3</sub>] > 40 mol%. This highlights the fact that E exhibits a non-linear dependence on composition—so that additive models are unlikely to offer good predictions for this system.

We now assess the validity of our topological model (Eq. (1)). To this end, we conduct a polynomial regression using as inputs the volumetric densities of BS and BB constraints ( $n_{\rm BS}$  and  $n_{\rm BB}$ ) shown in Fig. 1 and as output the simulated E values shows in Fig. 2a. This allows us to determine the typical energies of BS and BB constraints ( $\varepsilon_{\rm BS}$  and  $\varepsilon_{\rm BB}$ ) as fitting parameters. We find  $\varepsilon_{\rm BS}=2.82\,\rm eV$  and  $\varepsilon_{\rm BB}=1.78\,\rm eV$ . These values have the same order of magnitude as typical interatomic bond energies in silicate glasses [49]. As expected, we find that  $\varepsilon_{\rm BS}>\varepsilon_{\rm BB}$ , in agreement with the fact that the free energy of BS constraints is larger than that of BB constraints [23,46]. A more detailed polynomial regression using each type of constraints as independent inputs does not significantly improve the quality of the fit and further suggests that all the BS (and BB) constraints contribute to increasing the Young's modulus with a fairly similar energy "weight"  $\varepsilon$ .

Fig. 2b shows the *E* values predicted by Eq. (1). Overall, we find that the *E* values predicted by Eq. (1) agree well with the simulated values (see also Fig. 3a), although our topological model tends to slightly underpredict the Young's modulus of select calcium aluminate glasses on the CaO–Al<sub>2</sub>O<sub>3</sub> joint. Although the simulated values are here used to parameterize the  $\varepsilon_{\rm BS}$  and  $\varepsilon_{\rm BB}$  coefficients in Eq. (1), it is nevertheless striking that the complex compositional dependence of the Young's modulus of CAS glasses can be well reproduced with only two fitting parameters. We also note that our topological model does not keep the memory of the "noise" present in the MD data, which suggests that the model is not overfitted.

As a final validation of our model, Fig. 3b and c show a comparison between the Young's modulus predictions from our topological model (Eq. (1)), the simulation data, and available experimental data [50–61] for two joints, viz.,  $[SiO_2] = 60\%$  and  $[CaO] = [Al_2O_3]$ . These two series specifically aim to investigate (i) the effect of the degree of polymerization of the network (i.e., fraction of non-bridging oxygen) and (ii) the effect of network-forming atoms (i.e., Si vs. Al) at constant degree of depolymerization (i.e., in fully charge-compensated glasses). We note that our TCT model tends to slightly under- and over-estimate the Young's modulus of Ca- and Si-rich glasses, respectively—which is reminiscent of the predictions of the MD simulations. Nevertheless, we observe a good overall agreement between simulated data, topological predictions, and experimental data. In contrast, we find that the MM model systematically underestimates E and does not properly capture

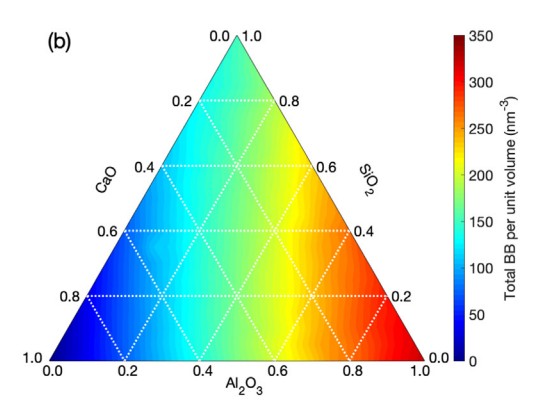


Fig. 1. Ternary diagram showing the volumic density of (a) bond-stretching (BS) and (b) bond-bending (BB) constraints as a function of composition in the  $CaO-Al_2O_3-SiO_2$  glass system.

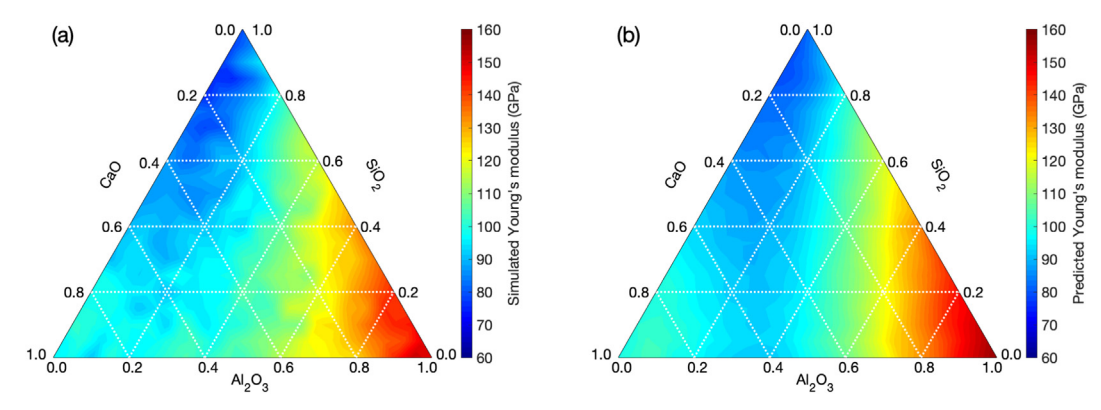


Fig. 2. Ternary diagram showing the Young's modulus values (a) computed by high-throughput molecular dynamics and (b) predicted by our topological model as a function of composition in the CaO-Al<sub>2</sub>O<sub>3</sub>-SiO<sub>2</sub> glass system.

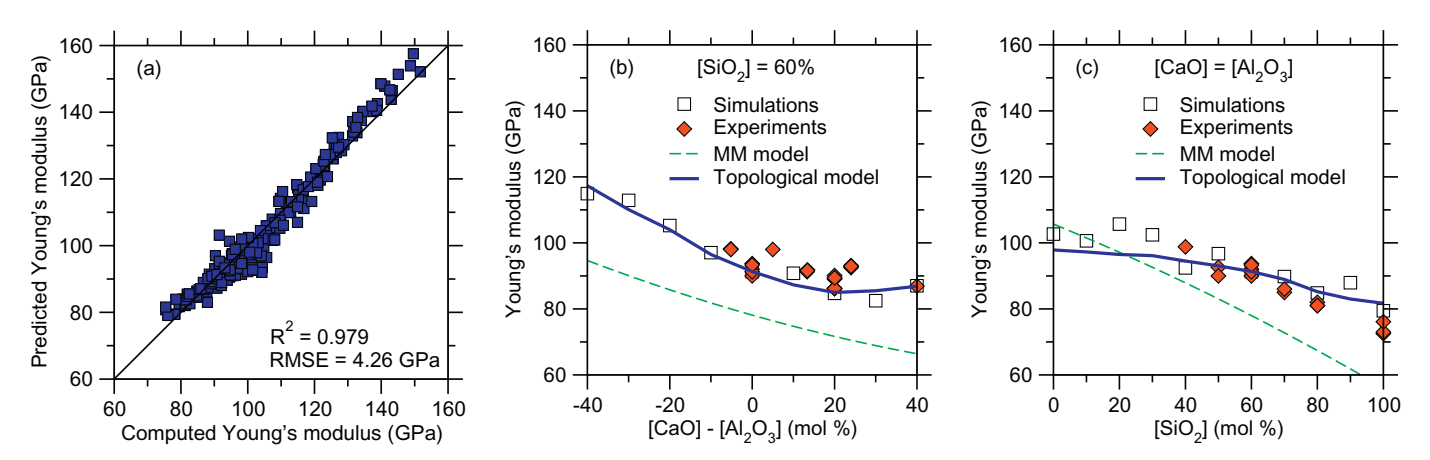


Fig. 3. (a) Comparison between the Young's modulus values predicted by our topological model (Eq. (1)) and computed by molecular dynamics simulations. We obtain a coefficient of determination  $R^2 = 0.979$  and a root mean squared error (RMSE) of 4.26 GPa. Comparison between the Young's modulus values computed by molecular dynamics simulations, predicted by our topological model, and predicted by the Makishima–Mackenzie (MM) model for the series of compositions (b)  $(CaO)_x(Al_2O_3)_{40-x}(SiO_2)_{60}$  and (c)  $(CaO)_x(Al_2O_3)_x(SiO_2)_{100-2x}$ . The data are compared with select available experimental data [50–61].

the non-linear nature of the Young's modulus data. Overall, these results strongly support the ability of our new topological model to offer reliable predictions of Young's modulus values over the entire CAS ternary domain.

#### 5. Conclusions

In summary, the results presented herein demonstrate that the Young's modulus of aluminosilicate glasses can be accurately predicted based on the volumetric densities of BS and BB topological constraints. As such, topological constraint theory offers a powerful framework to accelerate the design of new glass formulations with tailored stiffness. The atomistic origin of the energy coefficients  $\varepsilon_{\rm BS}$  and  $\varepsilon_{\rm BB}$  and whether their values depend on the considered glass system should be investigated in future work.

## Acknowledgements

This work was supported by the National Science Foundation under Grants No. 1562066, 1762292, 1826420, and 1826050. M.M.S. acknowledges support from the Independent Research Fund Denmark under Grant No. 8105-00002.

#### References

 L. Wondraczek, J.C. Mauro, J. Eckert, U. Kühn, J. Horbach, J. Deubener, T. Rouxel, Towards ultrastrong glasses, Adv. Mater. 23 (2011) 4578–4586, https://doi.org/10. 1002/adma.201102795.

- [2] J.C. Mauro, E.D. Zanotto, Two centuries of glass research: historical trends, current status, and grand challenges for the future, Int. J. Appl. Glas. Sci. 5 (2014) 313–327, https://doi.org/10.1111/ijag.12087.
- [3] J.C. Mauro, Grand challenges in glass science, Front. Mater. 1 (2014) 20, https://doi.org/10.3389/fmats.2014.00020.
- [4] J.C. Mauro, C.S. Philip, D.J. Vaughn, M.S. Pambianchi, Glass science in the United States: current status and future directions, Int. J. Appl. Glas. Sci. 5 (2014) 2–15, https://doi.org/10.1111/jjag.12058.
- [5] D.A. Krohn, A.R. Cooper, Strengthening of glass fibers: I, cladding \*, J. Am. Ceram. Soc. 52 (1969) 661–664, https://doi.org/10.1111/j.1151-2916.1969.tb16072.x.
- [6] A.R. Cooper, D.A. Krohn, Strengthening of class fibers: 11, ion exchange \*, J. Am. Ceram. Soc. 52 (1969) 665–669, https://doi.org/10.1111/j.1151-2916.1969. tb16073.x.
- [7] Z. Tang, N.P. Lower, P.K. Gupta, C.R. Kurkjian, R.K. Brow, Using the two-point bend technique to determine failure stress of pristine glass fibers, J. Non-Cryst. Solids 428 (2015) 98–104, https://doi.org/10.1016/j.jnoncrysol.2015.08.005.
- [8] T. Rouxel, Designing glasses to meet specific mechanical properties, Challenging Glass: Conference on Architectural and Structural Applications of Glass, Faculty of Architecture, Delft University of Technology, May 2008, IOS Press, 2008, p. 39.
- [9] T. Rouxel, Elastic properties of glasses: a multiscale approach, C. R. Mécanique. 334 (2006) 743–753, https://doi.org/10.1016/j.crme.2006.08.001.
- [10] T. Rouxel, Elastic properties and short-to medium-range order in glasses, J. Am. Ceram. Soc. 90 (2007) 3019–3039, https://doi.org/10.1111/j.1551-2916.2007. 01945.x.
- [11] J.C. Mauro, Decoding the glass genome, Curr. Opinion Solid State Mater. Sci. 22 (2018) 58-64. https://doi.org/10.1016/j.cossms.2017.09.001.
- [12] A. Makishima, J.D. Mackenzie, Direct calculation of Young's moidulus of glass, J. Non-Cryst. Solids 12 (1973) 35–45, https://doi.org/10.1016/0022-3093(73) 90053-7.
- [13] A. Makishima, J.D. Mackenzie, Calculation of bulk modulus, shear modulus and Poisson's ratio of glass, J. Non-Cryst. Solids 17 (1975) 147–157, https://doi.org/10. 1016/0022-3093(75)90047-2.
- [14] A.I. Priven, Methods of prediction of glass properties from chemical compositions, Glasses and the Glass Transition, John Wiley & Sons, Ltd, 2011, pp. 255–309, https://doi.org/10.1002/9783527636532.ch7.
- [15] K. Yang, X. Xu, B. Yang, B. Cook, H. Ramos, M. Bauchy, Prediction of Silicate

- Glasses' Stiffness by High-Throughput Molecular Dynamics Simulations and Machine Learning, ArXiv:1901.09323 [Cond-Mat], http://arxiv.org/abs/1901.09323, (2019) (accessed January 29, 2019).
- [16] M. Plucinski, J.W. Zwanziger, Topological constraints and the Makishima–Mackenzie model, J. Non-Cryst. Solids 429 (2015) 20–23, https://doi. org/10.1016/j.jnoncrysol.2015.08.029.
- [17] J.C. Phillips, Topology of covalent non-crystalline solids. 1. Short-range order in chalcogenide alloys, J. Non-Cryst. Solids 34 (1979) 153–181, https://doi.org/10. 1016/0022-3093(79)90033-4.
- [18] J.C. Phillips, Topology of covalent non-crystalline solids II: medium-range order in chalcogenide alloys and as-Si-Ge, J. Non-Cryst. Solids 43 (1981) 37–77, https://doi. org/10.1016/0022-3093(81)90172-1.
- [19] M. Bauchy, Deciphering the atomic genome of glasses by topological constraint theory and molecular dynamics: a review, Comput. Mater. Sci. 159 (2019) 95–102, https://doi.org/10.1016/j.commatsci.2018.12.004.
- [20] J.C. Mauro, Topological constraint theory of glass, Am. Ceram. Soc. Bull. 90 (2011)
- [21] M. Bauchy, Topological constraints and rigidity of network glasses from molecular dynamics simulations, Am. Ceram. Soc. Bull. 91 (2012) 34–38A.
- [22] M.M. Smedskjaer, J.C. Mauro, Y. Yue, Prediction of glass hardness using temperature-dependent constraint theory, Phys. Rev. Lett. 105 (2010) 115503, https://doi. org/10.1103/PhysRevLett.105.115503.
- [23] P.K. Gupta, J.C. Mauro, Composition dependence of glass transition temperature and fragility. I. A topological model incorporating temperature-dependent constraints, J. Chem. Phys. 130 (2009), https://doi.org/10.1063/1.3077168 094503-094503-8.
- [24] J.C. Mauro, P.K. Gupta, R.J. Loucks, Composition dependence of glass transition temperature and fragility. II. A topological model of alkali borate liquids, J. Chem. Phys. 130 (2009), https://doi.org/10.1063/1.3152432 234503-234503-8.
- [25] M.F. Thorpe, Continuous deformations in random networks, J. Non-Cryst. Solids 57 (1983) 355–370, https://doi.org/10.1016/0022-3093(83)90424-6.
- [26] G. Bhattarai, S. Dhungana, B.J. Nordell, A.N. Caruso, M.M. Paquette, W.A. Lanford, S.W. King, Underlying role of mechanical rigidity and topological constraints in physical sputtering and reactive ion etching of amorphous materials, Phys. Rev. Mater. 2 (2018) 055602, https://doi.org/10.1103/PhysRevMaterials.2.055602.
- [27] Q. Su, S. King, L. Li, T. Wang, J. Gigax, L. Shao, W.A. Lanford, M. Nastasi, Microstructure-mechanical properties correlation in irradiated amorphous SiOC, Scr. Mater. 146 (2018) 316–320, https://doi.org/10.1016/j.scriptamat.2017.11. 053
- [28] S.W. King, L. Ross, W.A. Lanford, Narrowing of the Boolchand intermediate phase window for amorphous hydrogenated silicon carbide, J. Non-Cryst. Solids 499 (2018) 252–256, https://doi.org/10.1016/j.jnoncrysol.2018.07.045.
- [29] M.M. Paquette, B.J. Nordell, A.N. Caruso, M. Sato, H. Fujiwara, S.W. King, Optimization of amorphous semiconductors and low-/high-k dielectrics through percolation and topological constraint theory, MRS Bull. 42 (2017) 39–44, https://doi.org/10.1557/mrs.2016.297.
- [30] S. Plimpton, Fast parallel algorithms for short-range molecular dynamics, J. Comput. Phys. 117 (1995) 1–19, https://doi.org/10.1006/jcph.1995.1039.
- [31] M. Bouhadja, N. Jakse, A. Pasturel, Structural and dynamic properties of calcium aluminosilicate melts: a molecular dynamics study, J. Chem. Phys. 138 (2013) 224510, https://doi.org/10.1063/1.4809523.
- [32] M. Bouhadja, N. Jakse, A. Pasturel, Striking role of non-bridging oxygen on glass transition temperature of calcium aluminosilicate glass-formers, J. Chem. Phys. 140 (2014) 234507, https://doi.org/10.1063/1.4882283.
- [33] M. Bauchy, Structural, vibrational, and elastic properties of a calcium aluminosilicate glass from molecular dynamics simulations: the role of the potential, J. Chem. Phys. 141 (2014) 024507, https://doi.org/10.1063/1.4886421.
- [34] B. Wang, Y. Yu, Y.J. Lee, M. Bauchy, Intrinsic nano-ductility of glasses: the critical role of composition, Front. Mater. 2 (2015) 11, https://doi.org/10.3389/fmats. 2015.00011
- [35] Y. Yu, B. Wang, Y.J. Lee, M. Bauchy, Fracture Toughness of Silicate Glasses: Insights from Molecular Dynamics Simulations, in: Symposium UU – Structure-Property Relations in Amorphous Solids, (2015), https://doi.org/10.1557/opl.2015.50.
- [36] C.J. Fennell, J.D. Gezelter, Is the Ewald summation still necessary? Pairwise alternatives to the accepted standard for long-range electrostatics, J. Chem. Phys. 124 (2006) 234104, https://doi.org/10.1063/1.2206581.
- [37] X. Li, W. Song, K. Yang, N.M.A. Krishnan, B. Wang, M.M. Smedskjaer, J.C. Mauro, G. Sant, M. Balonis, M. Bauchy, Cooling rate effects in sodium silicate glasses: bridging the gap between molecular dynamics simulations and experiments, J. Chem. Phys. 147 (2017) 074501, https://doi.org/10.1063/1.4998611.
- [38] L. Martínez, R. Andrade, E.G. Birgin, J.M. Martínez, PACKMOL: a package for

- building initial configurations for molecular dynamics simulations, J. Comput. Chem. 30 (2009) 2157–2164, https://doi.org/10.1002/jcc.21224.
- [39] H. Liu, S. Dong, L. Tang, N.M.A. Krishnan, G. Sant, M. Bauchy, Effects of polydispersity and disorder on the mechanical properties of hydrated silicate gels, J. Mech. Phys. Solids 122 (2019) 555–565, https://doi.org/10.1016/j.jmps.2018.10.
- [40] A. Pedone, G. Malavasi, A.N. Cormack, U. Segre, M.C. Menziani, Insight into elastic properties of binary alkali silicate glasses; prediction and interpretation through atomistic simulation techniques, Chem. Mater. 19 (2007) 3144–3154, https://doi. org/10.1021/cm062619r.
- [41] M.M. Smedskjaer, Topological model for boroaluminosilicate glass hardness, Front. Mater. 1 (2014) 23, https://doi.org/10.3389/fmats.2014.00023.
- [42] M.M. Smedskjaer, J.C. Mauro, S. Sen, Y. Yue, Quantitative design of glassy materials using temperature-dependent constraint theory, Chem. Mat. 22 (2010) 5358–5365, https://doi.org/10.1021/cm1016799.
- [43] J.C. Mauro, A. Tandia, K.D. Vargheese, Y.Z. Mauro, M.M. Smedskjaer, Accelerating the design of functional glasses through modeling, Chem. Mater. 28 (2016) 4267–4277, https://doi.org/10.1021/acs.chemmater.6b01054.
- [44] Q. Zheng, Y. Yue, J.C. Mauro, Density of topological constraints as a metric for predicting glass hardness, Appl. Phys. Lett. 111 (2017) 011907, https://doi.org/ 10.1063/1.4991971.
- [45] M. Bauchy, M.J.A. Qomi, C. Bichara, F.-J. Ulm, R.J.-M. Pellenq, Rigidity transition in materials: hardness is driven by weak atomic constraints, Phys. Rev. Lett. 114 (2015) 125502, https://doi.org/10.1103/PhysRevLett.114.125502.
- [46] M. Bauchy, M. Micoulaut, Atomic scale foundation of temperature-dependent bonding constraints in network glasses and liquids, J. Non-Cryst. Solids 357 (2011) 2530–2537, https://doi.org/10.1016/j.jnoncrysol.2011.03.017.
- [47] M. Bauchy, M.J. Abdolhosseini Qomi, C. Bichara, F.-J. Ulm, R.J.-M. Pellenq, Nanoscale structure of cement: viewpoint of rigidity theory, J. Phys. Chem. C 118 (2014) 12485–12493, https://doi.org/10.1021/jp502550z.
- [48] J.A. Tossell, J. Horbach, O Triclusters revisited: classical MD and quantum cluster results for glasses of composition Al2O3\$-SiO2, J. Phys. Chem. B 109 (2005) 1794–1797, https://doi.org/10.1021/jp0454873.
- [49] A.K. Varshneya, Fundamentals of Inorganic Glasses, Academic Press Inc, 1993.
- [50] R.J. Eagan, J.C. Swearekgen, Effect of composition on the mechanical properties of Aluminosilicate and borosilicate glasses, J. Am. Ceram. Soc. 61 (1978) 27–30, https://doi.org/10.1111/j.1151-2916.1978.tb09222.x.
- [51] C. Ecolivet, P. Verdier, Proprietes elastiques et indices de refraction de verres azotes, Mater. Res. Bull. 19 (1984) 227–231, https://doi.org/10.1016/0025-5408(84)90094-1.
- [52] S. Inaba, S. Todaka, Y. Ohta, K. Morinaga, Equation for estimating the Young,s modulus, shear modulus and Vickers hardness of aluminosilicate glasses, J. Jpn. Inst. Metals 64 (2000) 177–183. https://doi.org/10.2320/jinstmet1952.64.3 177
- [53] S. Inaba, S. Oda, K. Morinaga, Equation for estimating the thermal diffusivity, specific heat and thermal conductivity of oxide glasses, J. Jpn. Inst. Metals 65 (2001) 680–687, https://doi.org/10.2320/jinstmet1952.65.8\_680.
- [54] C. Weigel, C. Le Losq, R. Vialla, C. Dupas, S. Clément, D.R. Neuville, B. Rufflé, Elastic moduli of XAISiO4 aluminosilicate glasses: effects of charge-balancing cations, J. Non-Cryst. Solids 447 (2016) 267–272, https://doi.org/10.1016/j. inoncrysol.2016.06.023.
- [55] J. Rocherulle, C. Ecolivet, M. Poulain, P. Verdier, Y. Laurent, Elastic moduli of oxynitride glasses: extension of Makishima and Mackenzie's theory, J. Non-Cryst. Solids 108 (1989) 187–193, https://doi.org/10.1016/0022-3093(89)90582-6.
- [56] M. Yamane, M. Okuyama, Coordination number of aluminum ions in alkali-free alumino-silicate glasses, J. Non-Cryst. Solids 52 (1982) 217–226, https://doi.org/ 10.1016/0022-3093(82)90297-6.
- [57] S. Sugimura, S. Inaba, H. Abe, K. Morinaga, Compositional dependence of mechanical properties in aluminosilicate, borate and phosphate glasses, J. Ceram. Soc. Jpn. 110 (2002) 1103–1106, https://doi.org/10.2109/jcersj.110.1103.
- [58] T.M. Gross, M. Tomozawa, A. Koike, A glass with high crack initiation load: role of fictive temperature-independent mechanical properties, J. Non-Cryst. Solids 355 (2009) 563–568, https://doi.org/10.1016/j.jnoncrysol.2009.01.022.
- [59] I. Yasui, F. Utsuno, Material design of glasses based on database INTERGLAD, in: M. Doyama, J. Kihara, M. Tanaka, R. Yamamoto (Eds.), Computer Aided Innovation of New Materials II, Elsevier, Oxford, 1993, pp. 1539–1544, https://doi.org/10. 1016/B978-0-444-89778-7.50147-X.
- [60] L.-G. Hwa, K.-J. Hsieh, L.-C. Liu, Elastic moduli of low-silica calcium alumino-silicate glasses, Mater. Chem. Phys. 78 (2003) 105–110, https://doi.org/10.1016/S0254-0584(02)00331-0.
- [61] N.P. Bansal, R.H. Doremus, Handbook of Glass Properties, Elsevier, 2013.